



Multi3_

A cubic approach to Dark Matter



Enrico Borriello

Università degli Studi di Napoli "Federico II"

Dark Matter Constraints from galactic radio observations

Summary

- **Part I:** Constraints from our Galaxy (GC excluded)
- **Part II:** Constraints from external galaxies
- **Part III:** Constraints from the Galactic Center

Constraints from our Galaxy (GC excluded)

- We perform an **all-sky analysis**, covering the $15^\circ \times 15^\circ$ region surrounding the GC.
- We calculate the continuum radio emission due to DM annihilation as the sum of the **halo + clumps** components.
- We confront the expected radio flux with observations in the frequency range 0.1 GHz – 23 GHz and put **constraints** in the $m_\chi - \langle \sigma_{\text{A}} v \rangle$ plain.

Electrons Equilibrium Distribution

Dark matter annihilation injects electrons in the galaxy at the **constant rate**

$$Q(E_e, r) = \frac{1}{2} \left(\frac{\rho(r)}{m_\chi} \right)^2 \langle \sigma_A v \rangle \frac{dN_e}{dE_e}$$

The injected electrons lose energy in the interstellar medium and diffuse away from the production site:

$$\frac{\partial}{\partial t} \frac{dn_e}{dE_e} = \vec{\nabla} \cdot \left[K(E_e, r) \vec{\nabla} \frac{dn_e}{dE_e} \right] + \frac{\partial}{\partial E_e} \left[b(E_e, r) \vec{\nabla} \frac{dn_e}{dE_e} \right] + Q(E_e, r)$$

The diffusion length of electrons is generally of the order of a kpc thus for the diffuse signal generated all over the galaxy, **spatial diffusion** can be safely **neglected**. This is not the case for the signal coming from a single clump for which the emitting region is much smaller than a kpc.

Electrons Equilibrium Distribution

Neglecting spatial diffusion, **steady state solution** reads

$$\frac{dn_e}{dE_e}(\vec{E}_e, \vec{r}) = \frac{\tau(\vec{r})}{E_e} \int_{E_e}^{m_e c^2} dE_e' Q(E_e', \vec{r})$$

where τ is the **cooling time** resulting from the sum of several energy loss processes. We only take into account **Synchrotron emission** and **Inverse Compton Scattering** (ICS) on the background photons (CMB and starlight)

$$\frac{1}{\tau} = \frac{1}{\tau_{\text{syn}}} + \frac{1}{\tau_{\text{ICS}}}$$

Other processes, like synchrotron self absorption, ICS on the synchrotron photons, e^+e^- annihilation, Coulomb scattering over the galactic gas and bremsstrahlung are generally slower.

$$\tau_{\text{syn}} = 4 \cdot 10^{17} \left(\frac{B}{\mu\text{G}} \right)^{-2} \left(\frac{E_e}{\text{GeV}} \right)^{-1} \text{ s}$$
$$\tau_{\text{ICS}} = 10^{16} \left(\frac{U_{\text{rad}}}{\text{eV/cm}^3} \right)^{-1} \left(\frac{E_e}{\text{GeV}} \right)^{-1} \text{ s}$$

Dark Matter Synchrotron Signal

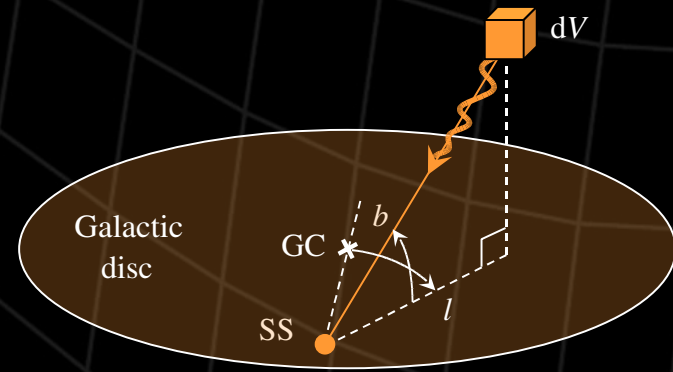
The synchrotron spectrum of an electron gyrating in a magnetic field has prominent peak at the resonance frequency

$$\nu = 3.4 \gamma \left(\frac{B}{\mu\text{G}} \right) \left(\frac{E_e}{\text{GeV}} \right)^2 \text{ MHz}$$

Using this **frequency peak** approximation, the **synchrotron emissivity** and the **differential flux** can be expressed as

$$j_\nu(\nu, \vec{r}) = \frac{dE_{\text{emit}}}{dV dt d\nu} = \frac{dn_e}{dE_e} (E_e(\nu), \vec{r}) b_{\text{syn}} (E_e(\nu), \vec{r}) \frac{dE_e(\nu)}{d\nu}$$

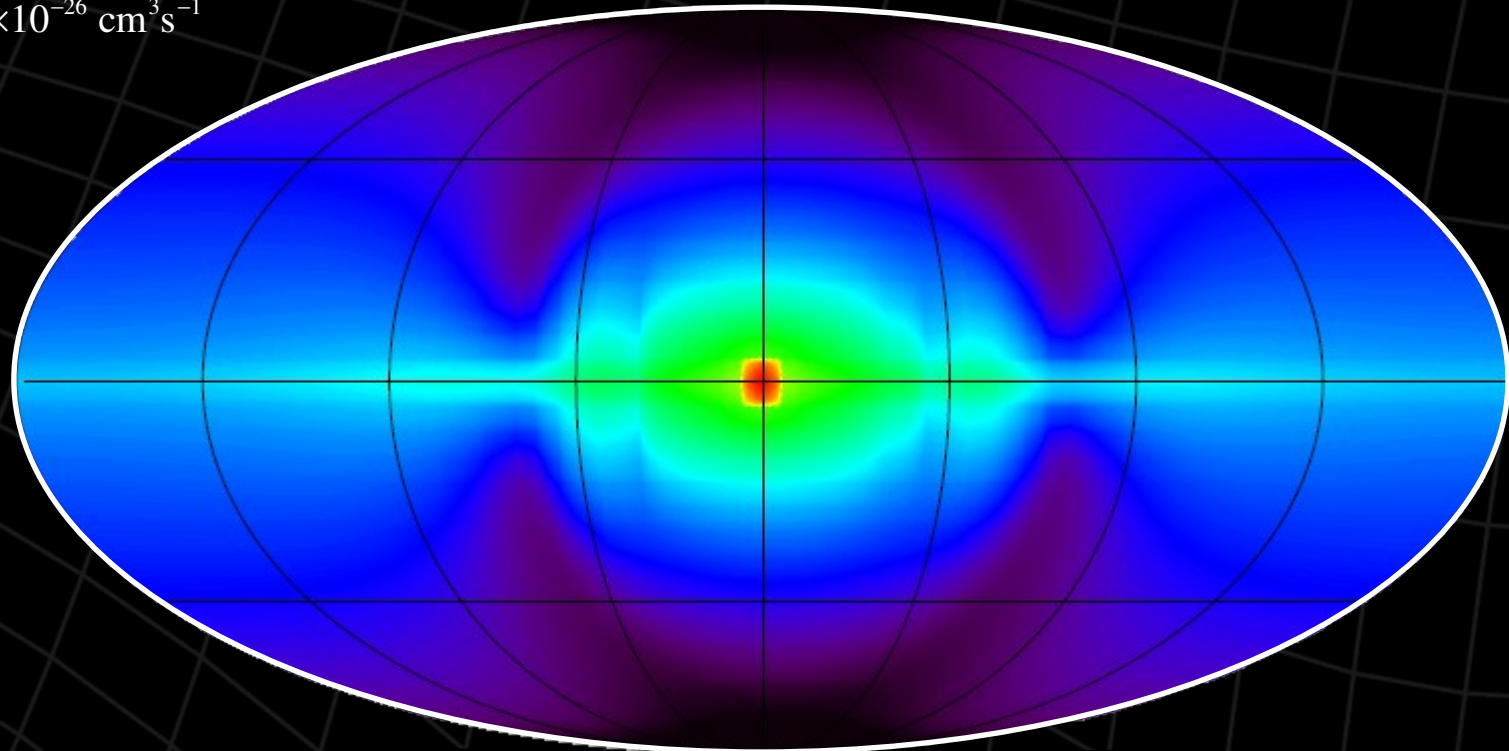
$$\frac{d^2 I_\nu}{dl db} = \frac{\cos b}{4\pi} \int_{\text{line of sight}} j_\nu(\nu, \vec{r}(s, l, b)) ds$$



Dark Matter Synchrotron Signal

$$m_\chi = 100 \text{ GeV}$$

$$\langle \sigma_A v \rangle = 3 \times 10^{-26} \text{ cm}^3 \text{ s}^{-1}$$



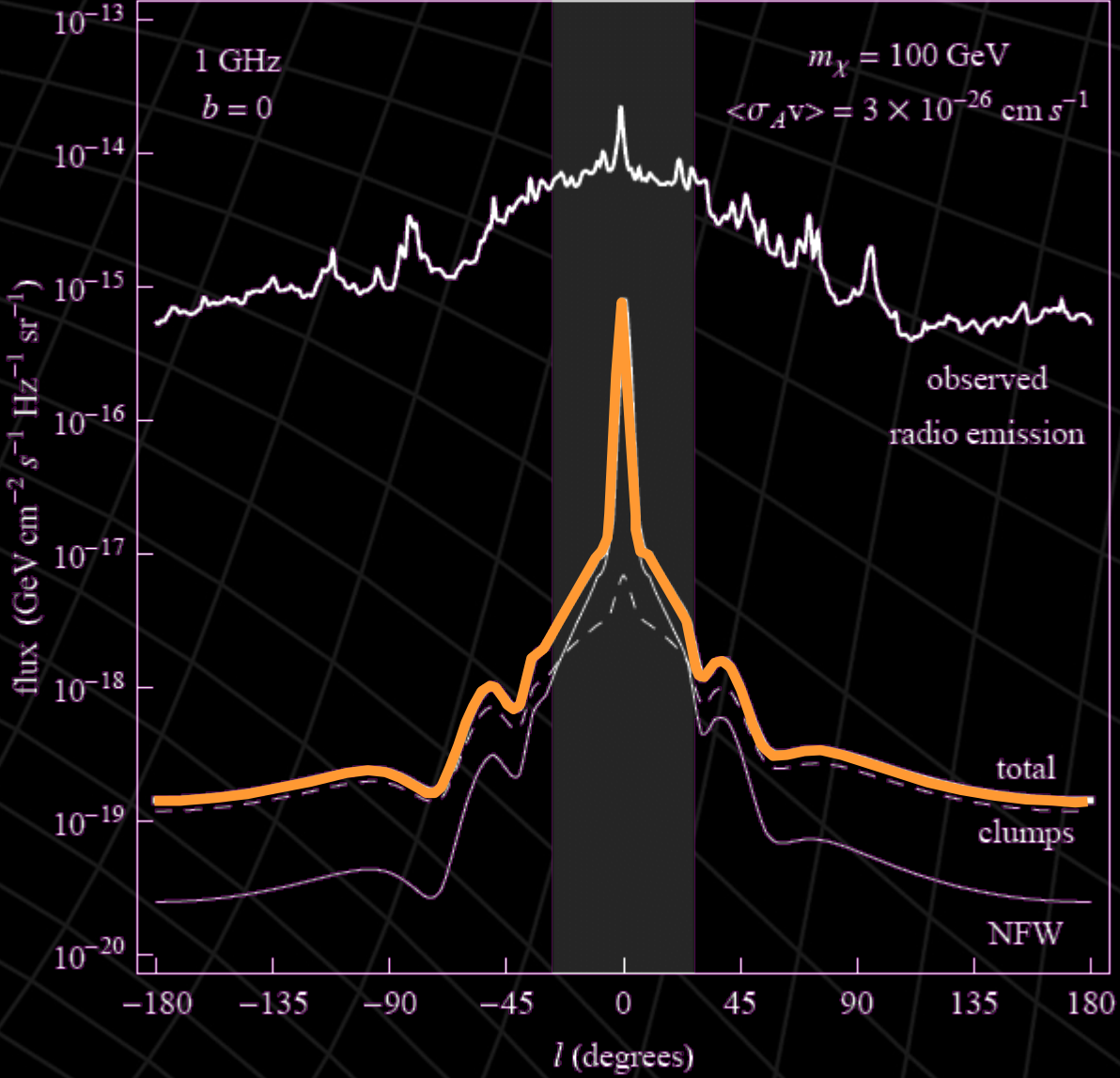
-21.1  -15.1

Log (GeV cm⁻³ s⁻¹ Hz⁻¹ sr⁻¹)

Sky map of the galactic radio signal generated by the DM smooth halo at the frequency of 1 GHz.

Dark Matter Synchrotron Signal

E. Borriello, A. Cuoco & G. Miele, Phys.Dev.D 79 (2009) 023518



The signal from **single bright clumps** offers only poor sensitivities because of diffusion effects which spread the electrons over large areas diluting the radio signal.

The **diffuse signal** from the halo and the unresolved clumps is instead relevant and can be compared to the radio astrophysical background to derive constraints on the DM mass and annihilation cross section.

Radio Foreground

Constraints on the DM emission are obtained comparing the expected diffuse emission from the “smooth halo” and the unresolved population of “clumps” with **all sky observation** in the radio band. In the frequency range between 100 MHz–100 GHz where the DM synchrotron signal is expected.

Contributions:

■ **CMB** that, thanks to the very sensitive multi-frequency survey by the WMAP (22.8, 33.0, 40.7, 60.8 and 93.5 GHz), can be modeled and removed from the observed radio galactic emission. Gold et al., arXIV:1001.4555

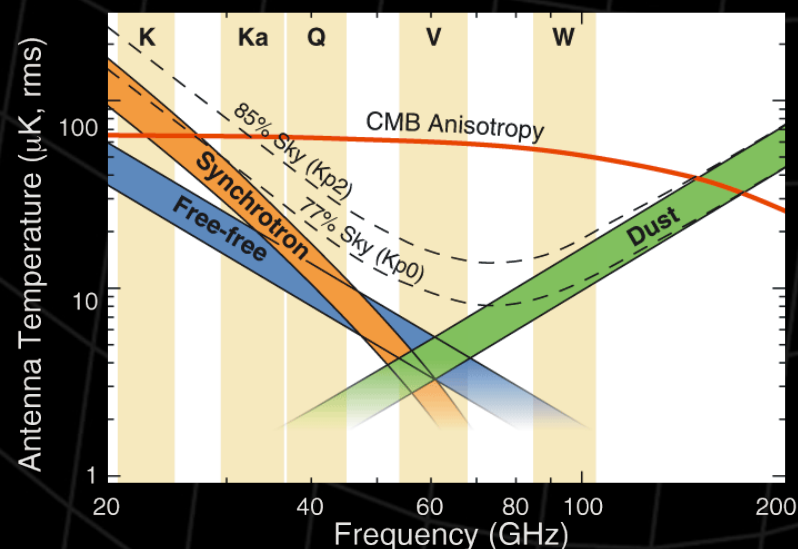
■ **Synchrotron** emission from relativistic electrons spiraling through the GMF.

Template: C.G.T. Haslam et al., A&A **100** (1981) 209.

■ **Free-free** emission: Thermal bremsstrahlung of non relativistic electrons on the galactic ionized gas. Template: D.P. Finkbeiner, ApJS **146** (2003) 407.

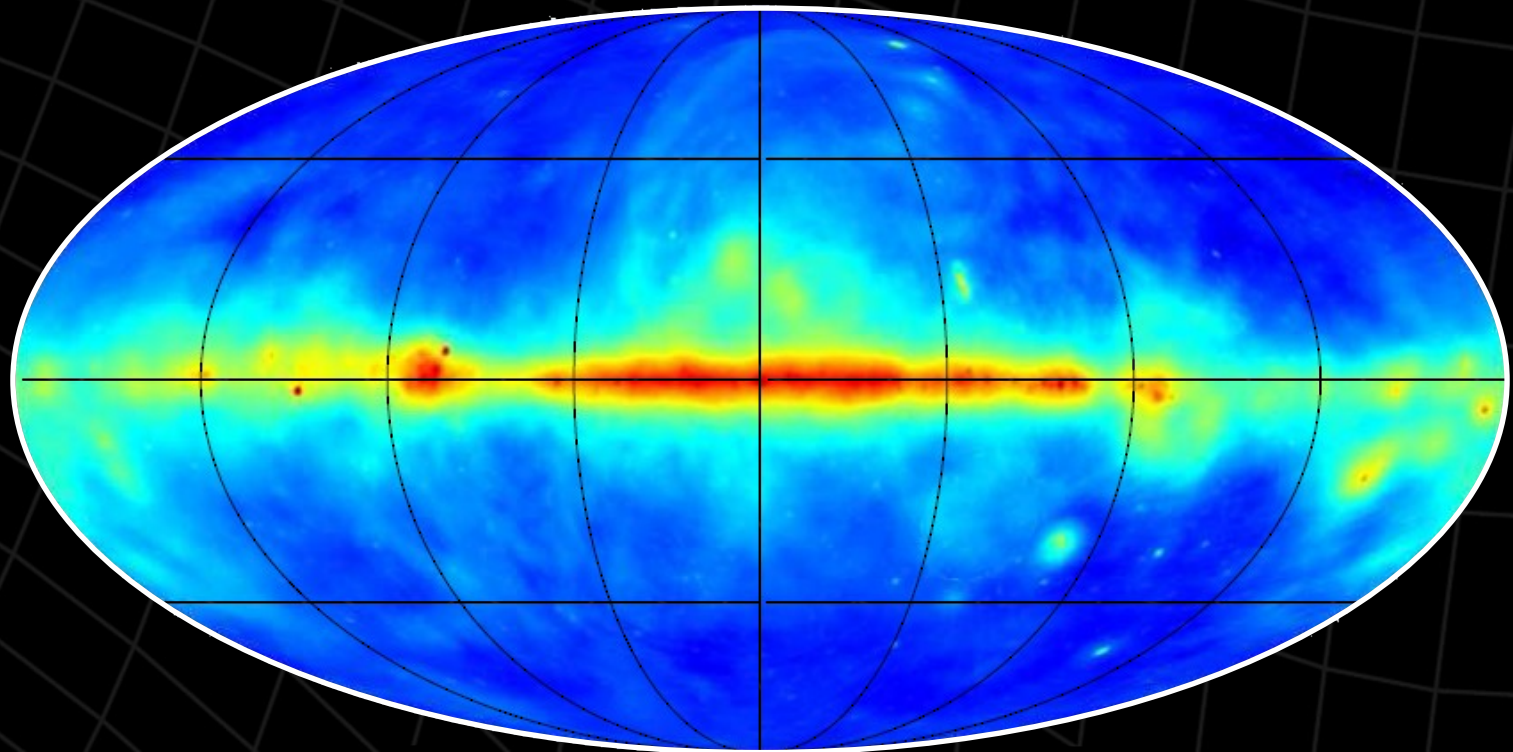
■ Emission from vibrational modes of thermal **dust** grains.


Template: D.P. Finkbeiner et al., ApJ **524** (1999) 867.



Radio Foreground

Radio Sky at 23 GHz
(CMB 'cleaned')



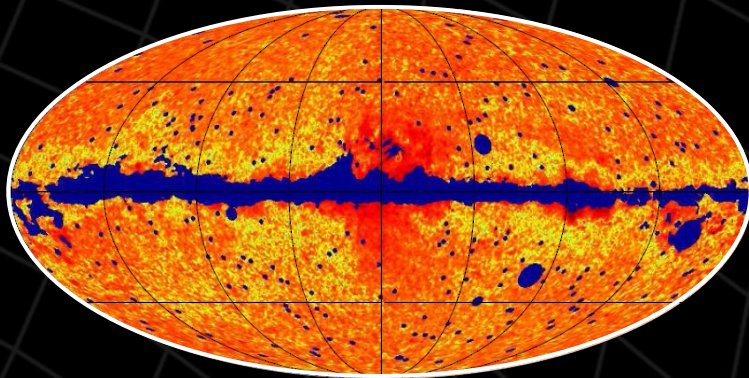
-18  -14
 $\text{Log}(\text{GeV cm}^{-3} \text{s}^{-1} \text{Hz}^{-1} \text{sr}^{-1})$

Radio Foreground

Model dependent approach:

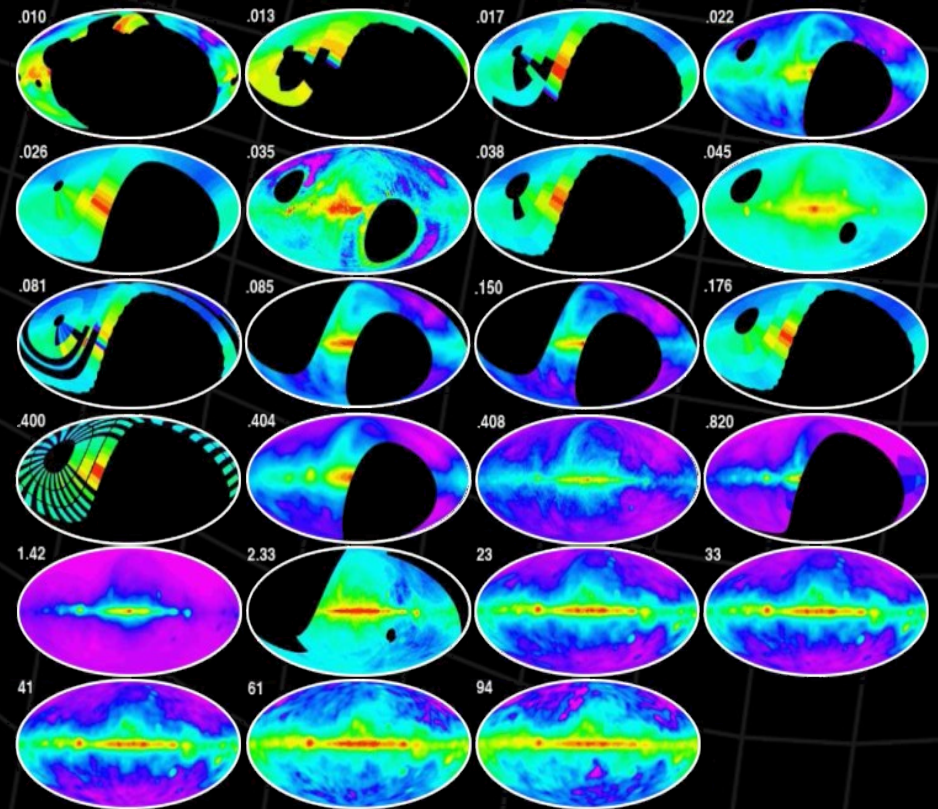
One can try to remove the foreground (WMAP Haze)

D.P. Finkbainer, arXiv:astro-ph/0409027
D. Hooper et al., Phys. Rev. D 76 (2007) 083012



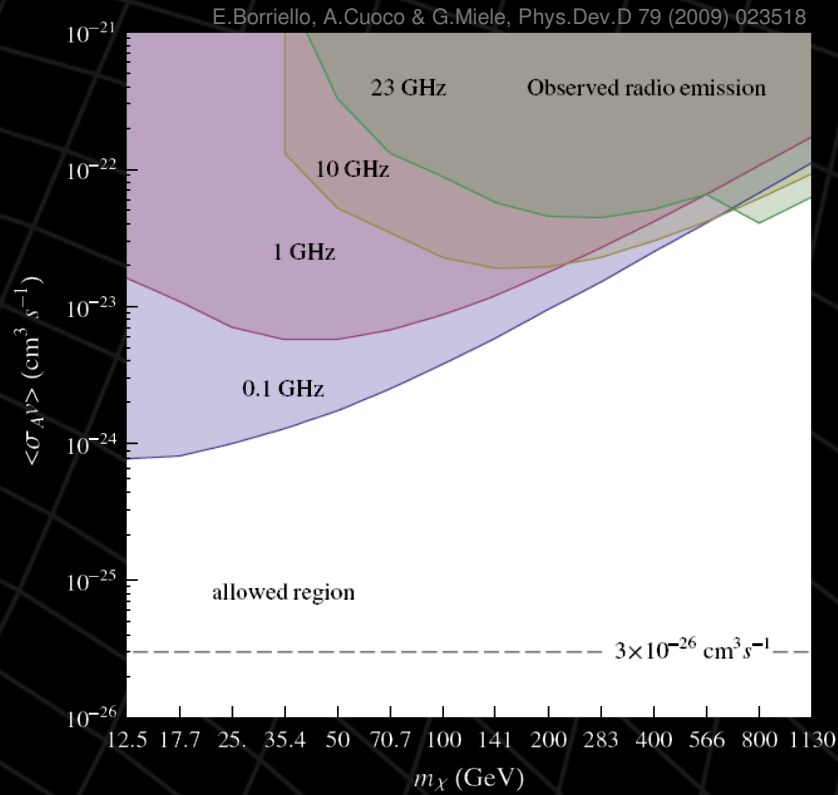
Our approach (conservative):

One can compare the DM signal with the observed radio emission where only the CMB is removed. We use the code of De Olivera Costa et al., where most of the radio survey observations in the range 10 MHz–100 GHz are collected and interpolated.

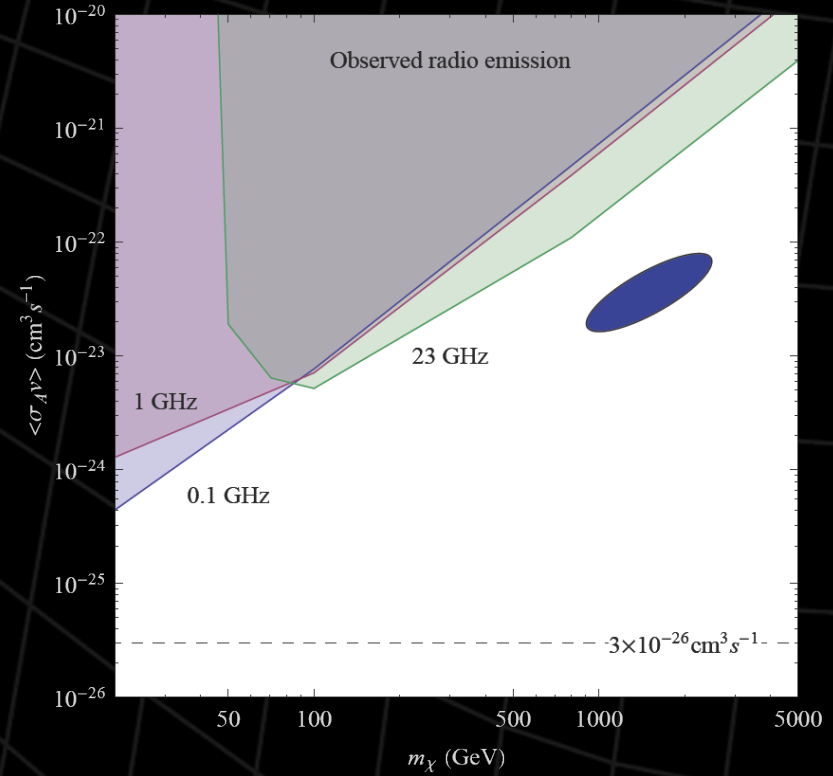


De Olivera Costa et al., arXiv:0802.1525 [astro-ph]

DM Annihilation Constraints

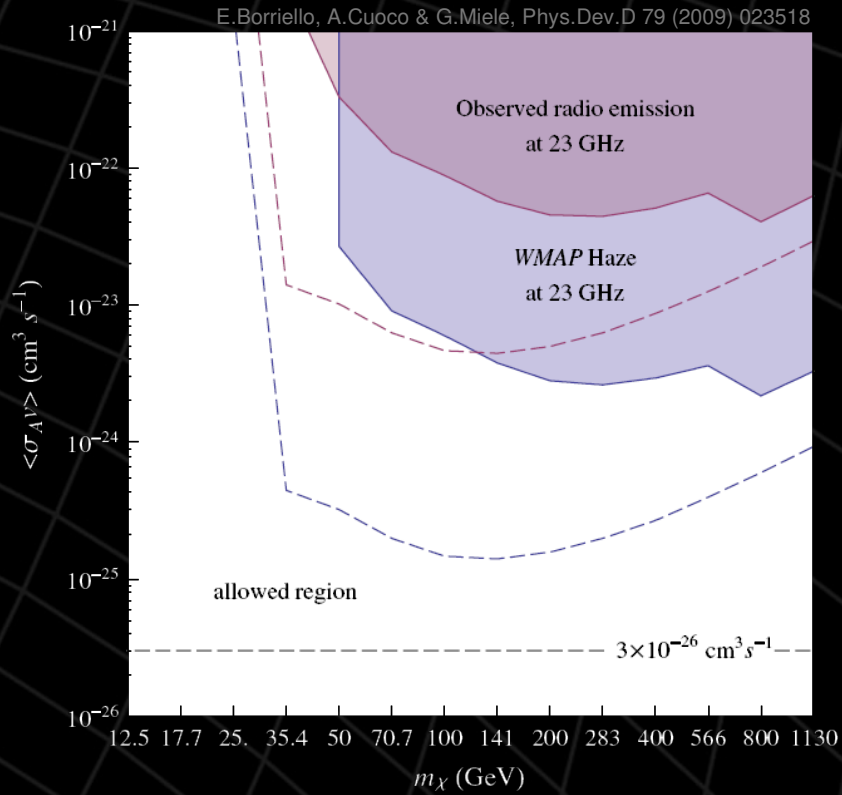


$$\chi\chi \rightarrow q\bar{q}$$

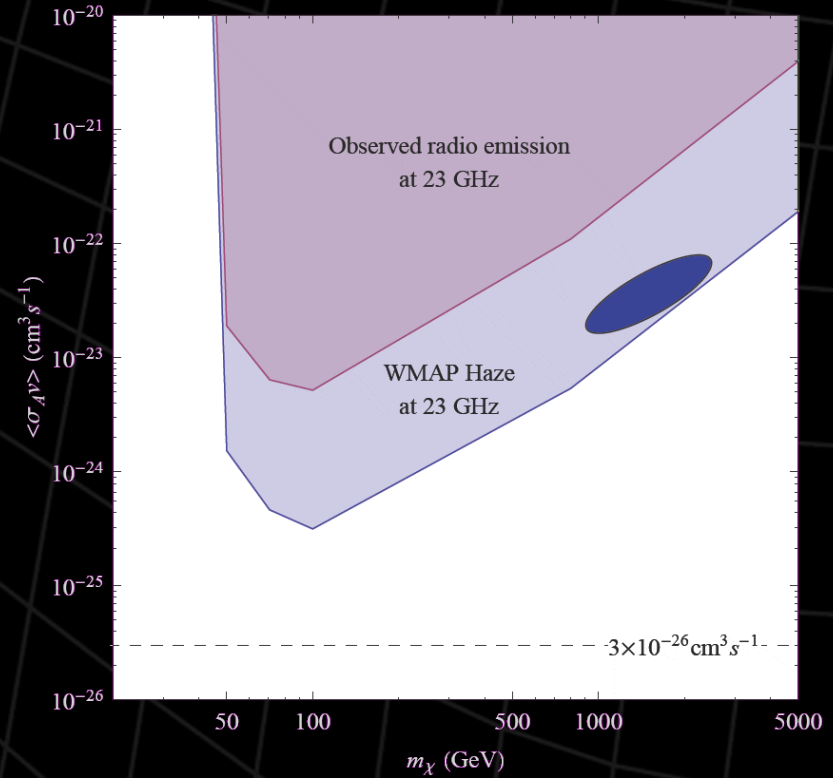


$$\chi\chi \rightarrow \mu^+\mu^-$$

DM Annihilation Constraints



$$\chi\chi \rightarrow q\bar{q}$$

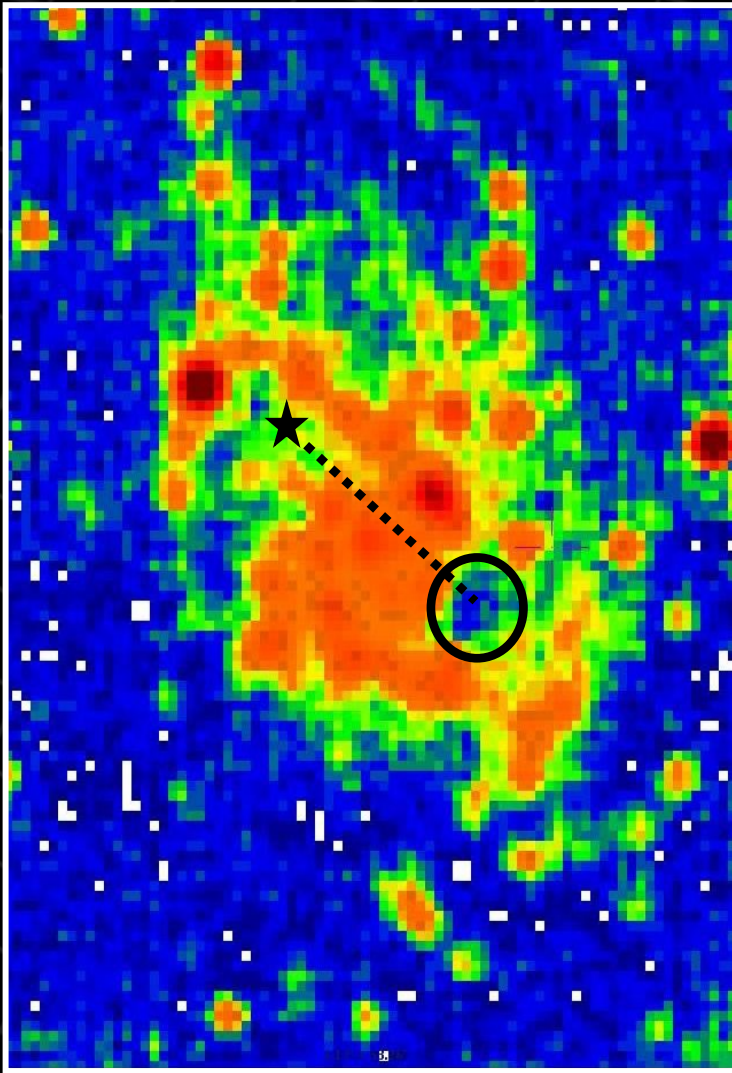


$$\chi\chi \rightarrow \mu^+\mu^-$$

Constraints from external galaxies

- Instead of calculating the integrate radio flux coming from the entire galaxy (a lot of uncertainties would be propagated on the final results) we could concentrate on a small region, for this could be well known from an astrophysical point of view.
- Our aim is to reduce the best we can the foreground contamination to the observed flux.

Radio cavities in external galaxies



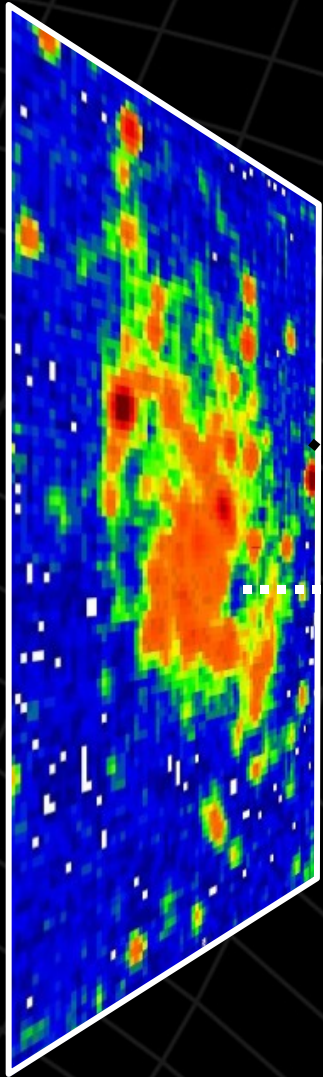
The presence of strong inhomogeneities in radio maps of galaxies is a common feature.

We expect them in the MW, too. We cannot see them because we share their position in the disc of the Galaxy.

The situation changes completely if we, instead, belong to a different galaxy, particularly if the external galaxy is placed “**face-on**” with respect to us.

This way we obtain the **lowest** possible value of **foreground contamination** on our results.

Radio cavities in external galaxies



The presence of strong inhomogeneities in radio maps of galaxies is a common feature.

We expect them in the MW, too. We cannot see them because we share their position in the disc of the Galaxy.

The situation changes completely if we, instead, belong to a different galaxy, particularly if the external galaxy is placed “**face-on**” with respect to us.

This way we obtain the **lowest** possible value of **foreground contamination** on our results.

The Triangulum Galaxy (M33)



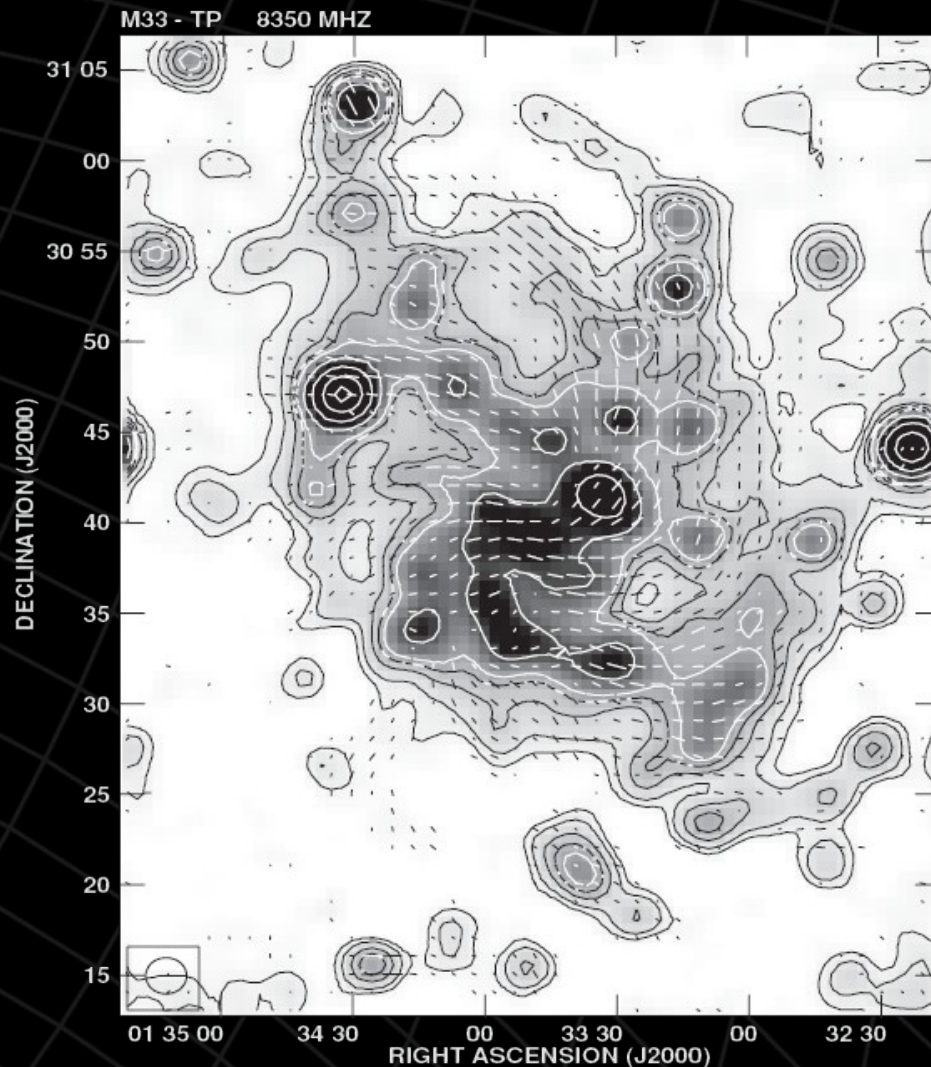
M33 is a **spiral galaxy** approximately 3 million light-years away (840 kpc). It is the **third largest galaxy** in the Local Group, after the Andromeda Galaxy and the Milky Way.

It has an inclination of **56°**, therefore its spiral structure is clearly visible.

It has been extensively studied at all wavelengths, from radio to X-rays.

© IAC/RGO/Malin

The Radio Cavity of M33



Radio map of M33 at 3.6 cm (8.35 GHz)

M33 possesses many regions characterized by a **low emissivity** at radio frequencies.

In particular there is a **Radio Cavity** located at only 2 kpc from the centre where the flux reaches its minimum.

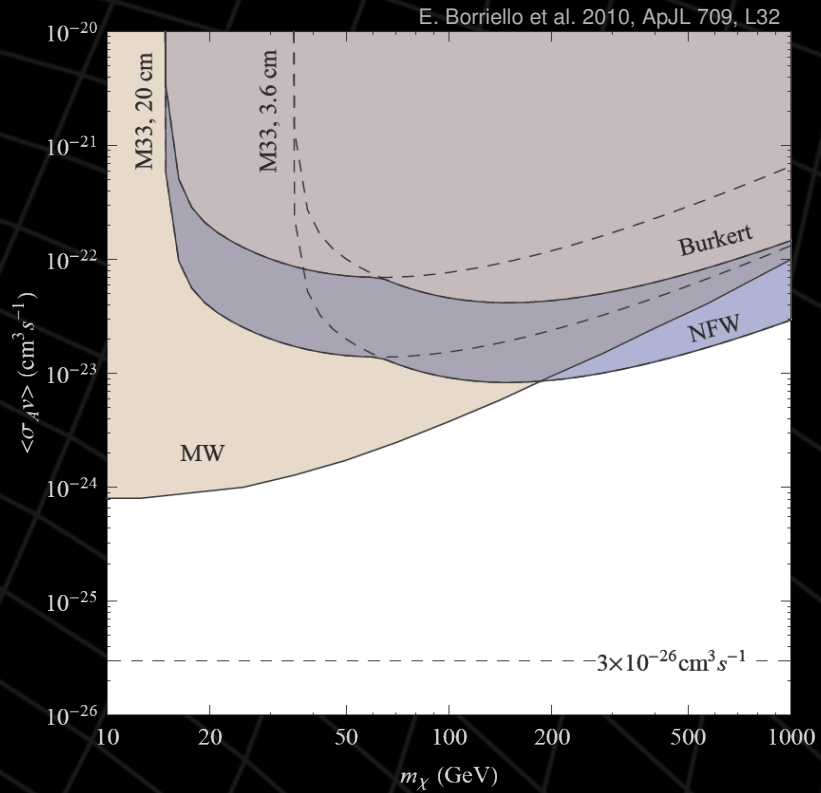
Mean magnetic field: 6.4 μG

Magnetic field in the cavity: **7.1 μG**

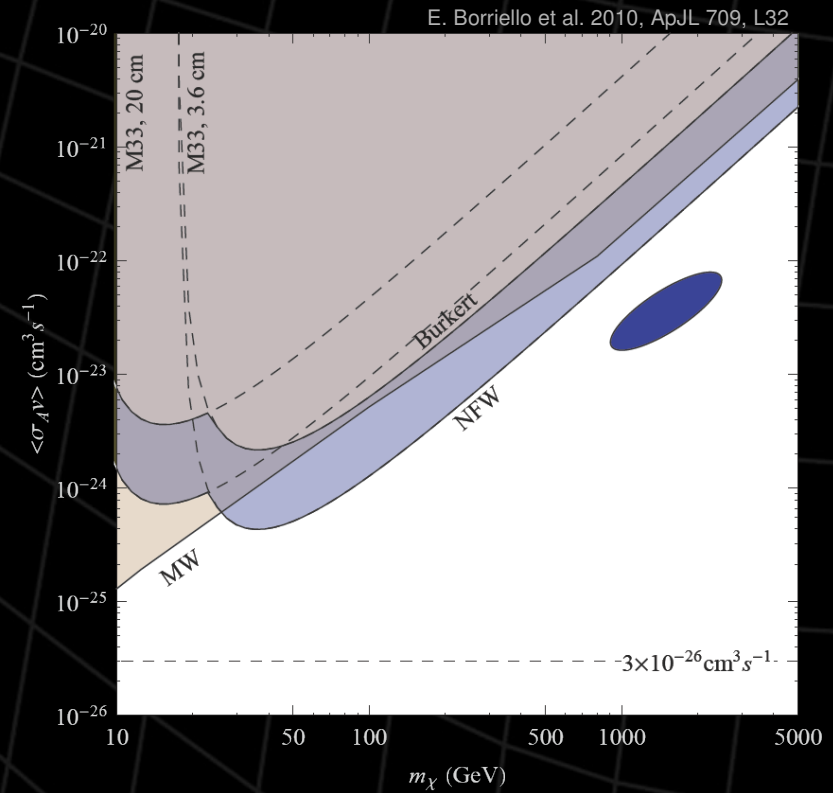
This Radio Cavity looks like the **ideal place** where to look for a DM signal.

F.S. Tabatabaei, M. Krause, R. Beck, *Astron. Astrophys.* **472** (2007) 785.

Radio constraints from M33



$$\chi\chi \rightarrow q\bar{q}$$



$$\chi\chi \rightarrow \mu^+\mu^-$$

Forecasts for ALMA (140 GHz)

A better scan of the radio cavity could lead to two improvements:

We could find a pixel from which we observe no flux (a flux comparable to the experimental sensitivity).

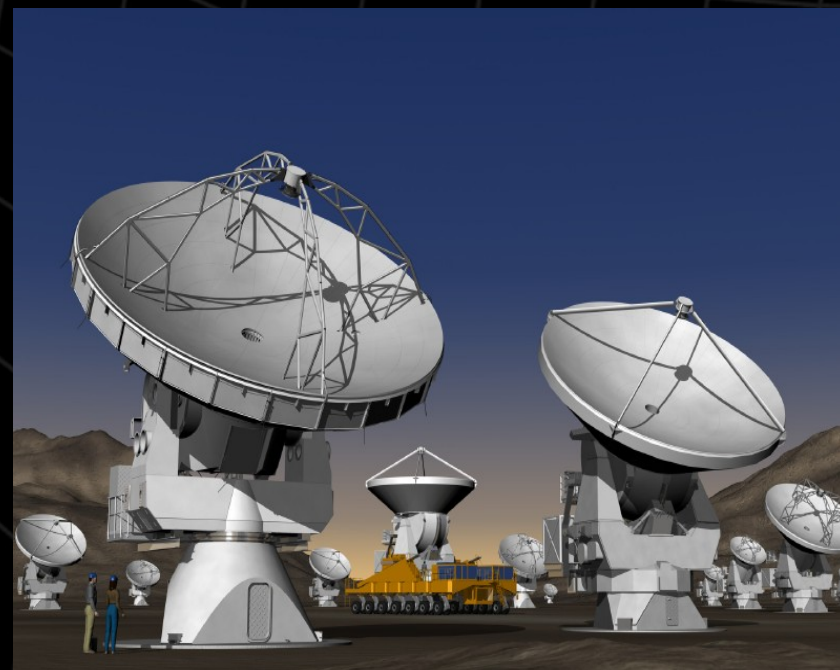
A spectral analysis of the different foreground contributions could lead to a foreground removal (at least around the least flux region).

Therefore, to test the potentiality of the method we deduce the bounds we would be able to put in the case of **“null detection”**.

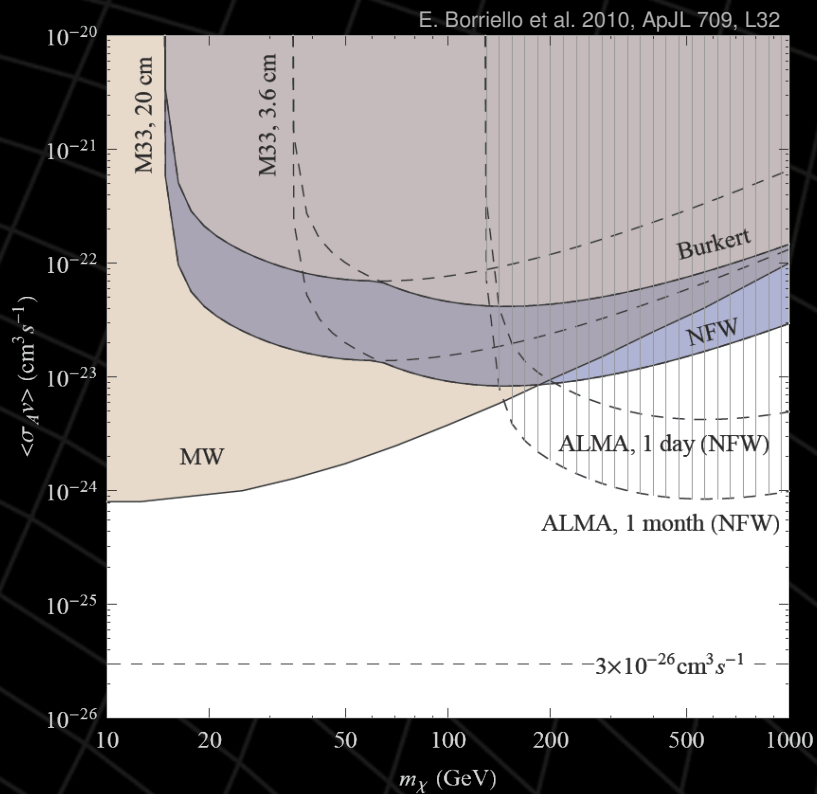
ALMA Sensitivity Goals for the 12 m Array

For an integration time of 60 seconds, a spectral resolution of 1 km s^{-1} , the RMS flux density, ΔS , and brightness temperature sensitivity, ΔT , with a 64 antenna array and maximum baseline, B_{max} , will be:

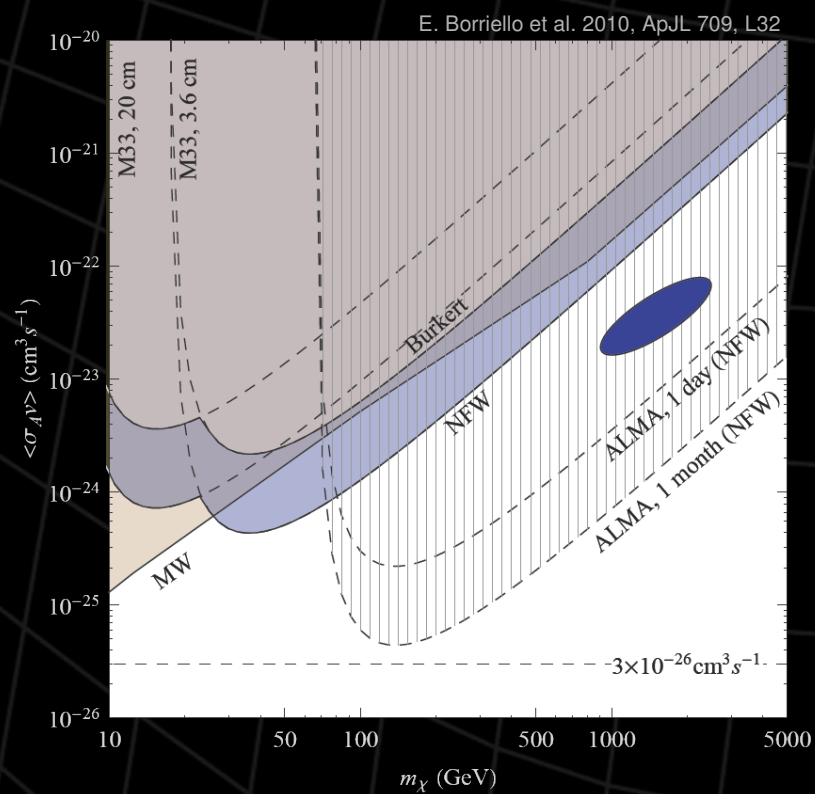
Frequency (GHz)	Continuum ΔS (mJy)	Spectral Line ΔS (mJy)	Beam (arcsec)	$B_{\text{max}} = 0.2 \text{ km}$		$B_{\text{max}} = 14.7 \text{ km}$		
				ΔT_{cont} (K)	ΔT_{line} (K)	Beam (arcsec)	ΔT_{cont} (K)	ΔT_{line} (K)
110	0.047	7.0	3.18	0.0005	0.070	0.038	3.3	482
140	0.055	7.1	2.50	0.0005	0.071	0.030	3.8	495
230	0.100	10.2	1.52	0.0010	0.104	0.018	6.9	709
345	0.195	16.3	1.01	0.0020	0.167	0.012	13.5	1128
409	0.296	22.6	0.86	0.0031	0.234	0.010	20.5	1569
675	1.042	62.1	0.52	0.0108	0.641	0.006	72.2	4305



Forecasts for ALMA (140 GHz)



$$\chi\chi \rightarrow q\bar{q}$$



$$\chi\chi \rightarrow \mu^+\mu^-$$

Constraints from the Galactic Center

- R.M. Crocker et al., Nature **463** (2010) 65
*A lower limit of **50 microgauss** for the magnetic field near the Galactic Centre*
- R.M. Crocker et al., arXiv:1002.0229
*Radio **and gamma-ray** constraints on dark matter annihilation in the Galactic center*

Lower limit for the magnetic field near the GC

$$\nu_b = \nu_b(n_H, B) \approx 1.7 \text{ GHz}$$

$$B \simeq B(n_H)$$

$$\frac{dN_e}{dE_e} \propto E_e^p$$

$$\frac{dn_e}{dE_e}(n_H, B, p)$$

$$F_\nu^{(brm+ICSS)}(n_H, B, p)$$

$$F_\nu^{(syn)}(n_H, B, p)$$

$$F_\nu^{(brm+ICSS)} \leq F_\nu^{(Hess)}$$

$$B \gtrsim 50 \mu\text{G}$$

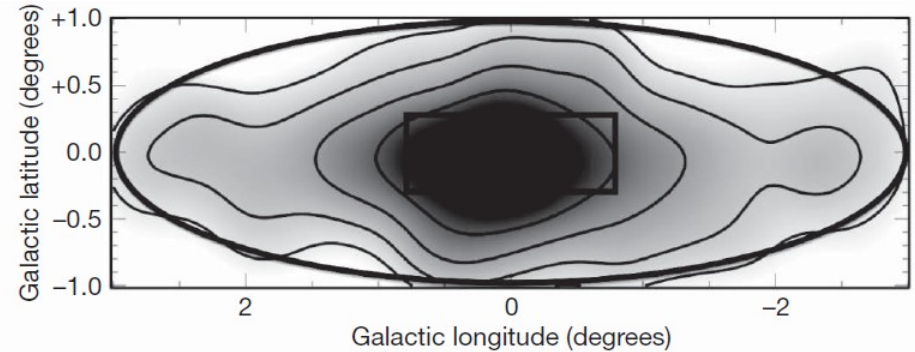
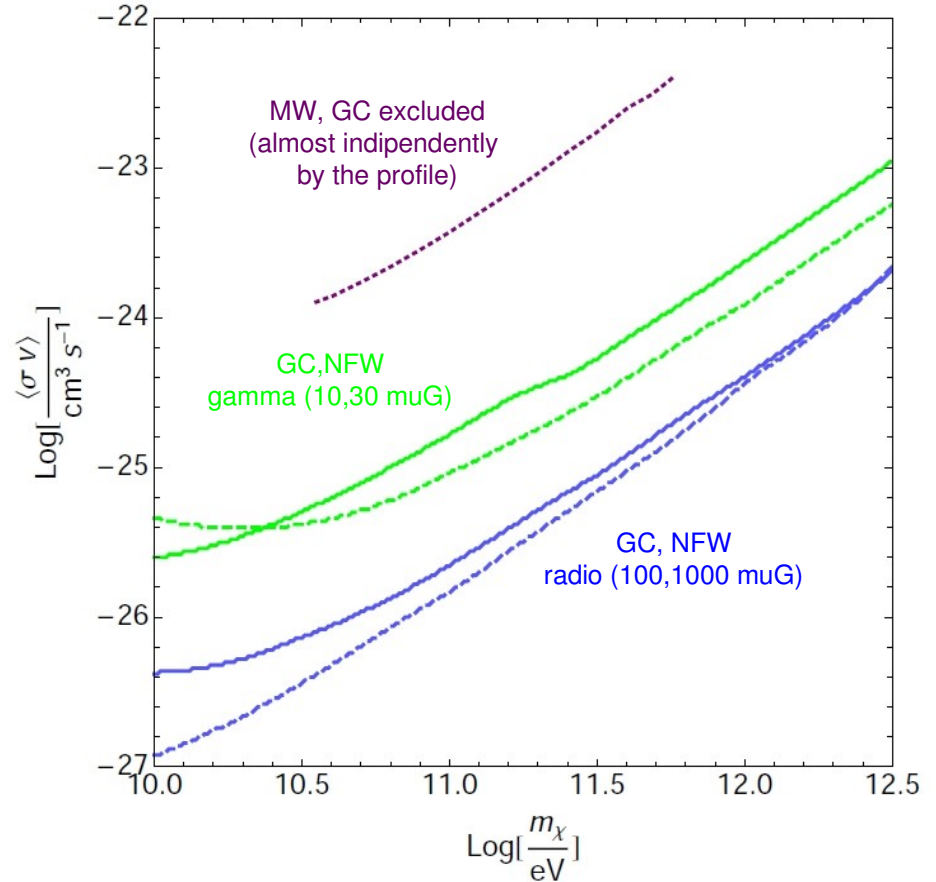
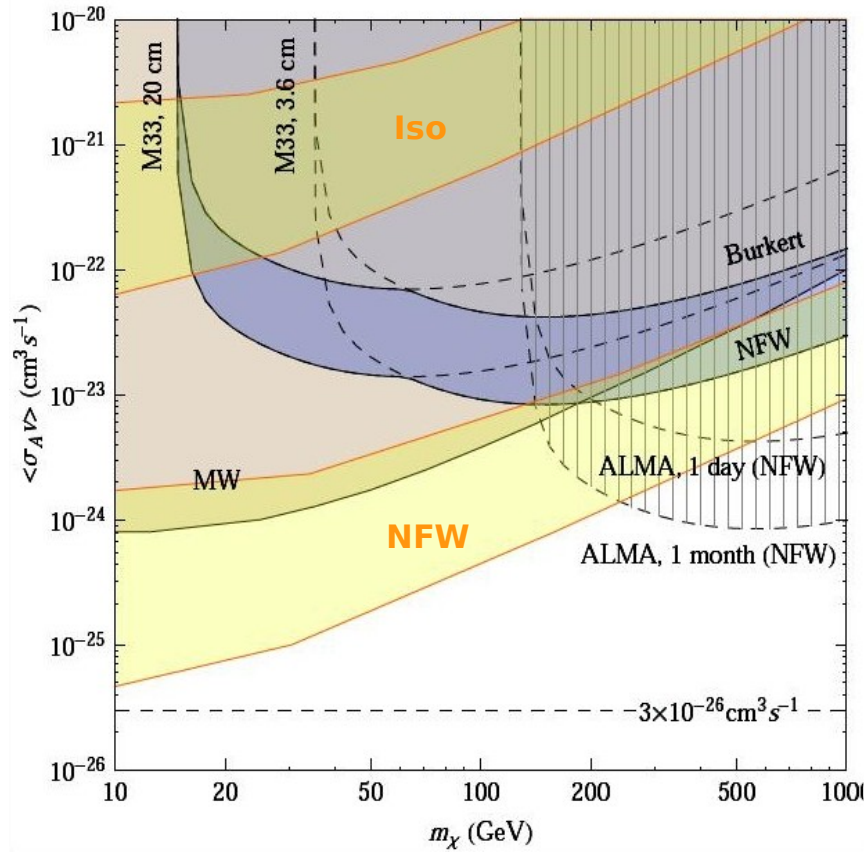


Figure 1 | Total intensity image of the region at 10 GHz. Radio map¹³ convolved to a resolution of $1.2^\circ \times 1.2^\circ$ with contours at 10, 20, 40, 80, 160 and 240 Jy per beam. (Native resolution and convolved images at $\nu \geq 1.4$ GHz are available in the Supplementary Information.) There is a striking constancy in the appearance of the radio structure from 74 MHz to at least 10 GHz (the large ellipse traces the diffuse, non-thermal radio emission region first identified at 74 and 330 MHz; ref. 6). The small rectangle delineates the region from which the HESS collaboration determines a diffuse \sim TeV γ -ray intensity⁸.

Constraints from the GC



Conclusions

Key elements to obtain good constrains from astrophysical observations at radio frequencies:

■ Intense magnetic field:

The GC should be the preferred region, but the dark matter density there is almost totally unknown. And the uncertainty is **squared**...

■ Low foreground contaminations:

- **LOFAR** is under construction. 10-250 MHz
- **SKA** is under design. 0.3-30 GHz
- **Planck** has started its second all sky survey. 30-900 GHz

These surveys will help in disentangling the various astrophysical contributions, hopefully leading to a better determination of the **Haze** and, thus, to a **model independent** improvement of these results.

Thank you for your attention =)